

Preparation and Characterization of PVDF/Silica Hybrid Membranes Containing Sulfonic Acid Groups

Dae Sik Kim,¹ Ho Bum Park,¹ Young Moo Lee,¹ Young Hoon Park,² Ji-Won Rhim³

¹National Research Laboratory for Membranes, School of Chemical Engineering, College of Engineering, Hanyang University, Seoul 133-791, Korea

²Department of Polymer Engineering, Suncheon National University, Suncheon, Korea

³Department of Chemical Engineering, Hannam University, 133 Ojung-Dong, Daeduk-gu, Daejeon 306-791, Korea

Received 24 July 2003; accepted 18 December 2003

DOI 10.1002/app.20451

Published online in Wiley InterScience (www.interscience.wiley.com).

ABSTRACT: Organic–inorganic hybrid membranes of poly(vinylidene fluoride)-cohexafluoropropylene (PVDF-HFP) and silica composites containing sulfonic acid groups were prepared via *in situ* polymerization of tetraethoxysilane (TEOS) and sulfosuccinic acid (SSA) using the sol-gel process. The membranes containing more sulfonic acid groups showed a higher vapor sorption and greater swelling behavior. The bound and free water content of the membrane is proportional to the SSA concentration. However, the hybrid membranes without SSA do not have free water. The ion conductivity of the membranes is proportional to the SSA concentration. Silica content in the hybrid membrane without SSA had great effect on their mechanical

properties. Tensile modulus and yield stress increased and yield strain and elongation at break decreased with increased silica content. However, in the case of the hybrid membrane containing SSA modulus, yield stress decreased and yield strain and elongation at break increased with increased silica content due to the weak interactions between the hydrophobic polymer chain and the hydrophilic group of SSA. © 2004 Wiley Periodicals, Inc. *J Appl Polym Sci* 93: 209–218, 2004

Key words: poly(vinylidene fluoride); silicas; membranes; ionomers; ion exchangers

INTRODUCTION

In recent years, hybrid organic–inorganic composites have attracted much attention because such hybrids may show controllable properties such as optical, electrical, and mechanical behaviors by combining the properties of both organic polymers and inorganic compounds.^{1–5} If these materials can be combined effectively, a new class of high performance or highly functional organic–inorganic hybrid materials could be obtained.⁶ In organic–inorganic hybrids, inorganic minerals precipitate *in situ* evenly in the organic polymer matrix, and the strong interaction between the organic polymer and inorganic mineral may result in a hybrid of markedly improved mechanical properties. The properties of a composite material depend on the properties of each component as well as on the phase morphology of composites and interfacial properties.

The reaction is divided into two steps. Hydrolysis and condensation of metal alkoxide leads to the formation of an inorganic network.^{7,8} On the basis of the interfacial interaction between the organic and inor-

ganic phases, the organic–inorganic hybrid materials can be classified into two distinct types.⁷ The first type is due to formation of extensive hydrogen bonding between the hybrid materials, and the second type has the components connected to each other by covalent bonds. Interaction between the organic polymer matrix and the inorganic mineral, for example, through hydrogen bonding, plays an important role in avoiding phase separation and yielding transparent free-standing films.⁶

Since the sol-gel process proceeds under mild conditions at low temperature and atmospheric pressure, thermally unstable organic polymers can be incorporated with inorganic materials to obtain organic–inorganic hybrids. Organic–inorganic hybrids of poly(vinyl acetate), acrylic resin, polyurethane, Nafion, poly(vinyl pyrrolidone), poly(methyl methacrylate), poly(imidesiloxane), and poly(vinylidene fluoride) (PVDF) have been reported.^{6,9,10} Starting materials for the sol-gel process are metal alkoxides and a small amount of acid or base as catalyst. Hybrids are prepared usually through a sol-gel process by incorporating organic polymers with alkoxysilanes, mainly tetramethoxysilane (TMOS) or tetraethoxysilane (TEOS).⁴

Saegusa¹¹ and Chujo et al.¹² obtained homogeneous transparent glass-like composites by the sol-gel process using silicon alkoxide and polyoxazoline. It is thought that the organic polymers of these composites

Correspondence to: Y. M. Lee (ymlee@hanyang.ac.kr).

have hydrogen bond acceptor groups and can form hydrogen bonds with silanol groups on silica.⁶

PVDF and its copolymers with other fluorocarbons are well known to have ferroelectric, piezoelectric, and pyroelectric properties and to crystallize easily on cooling from the melt. Their combination with SiO₂ may result in a large diversity of electroactive and mechanical properties.¹³

Because hydrophilic polymer materials swell in aqueous media, the membranes would lose their mechanical resistance if they were too hydrophilic. A compromise needs to be found for each type of application by balancing hydrophilicity against hydrophobicity. One way to do this is to copolymerize monomers with hydrophilic and hydrophobic groups.¹⁴ Several organic groups such as hydroxyl, amine, carboxylate, sulfonate, and quaternary ammonium can be used to impart hydrophilicity to a polymer.^{15,16} However, the procedures used to incorporate these hydrophilic groups in their structures are generally not simple and the reaction conditions are sometimes extreme.¹⁷ Thus, the synthesis of a sulfonated polymer using a monomer containing the sulfonic acid group is the most favorable way because of easy control of the degree of sulfonation and prevention of polymer decomposition.

The aim of this study is to provide the preparation and characterization of the modified hybrid membrane based on PVDF/silica and the possibility of the esterification between sulfosuccinic acid and hydrolyzed TEOS. In this study, the introduction of sulfonic acid group into PVDF membranes was achieved by the modifications of silica through esterification with sulfosuccinic acid (SSA) having a carboxylic acid group and silica having a Si-OH group induced from TEOS.

The mechanical properties as well as morphological features of PVDF/SiO₂ hybrid membranes containing sulfonic acid groups produced via the sol-gel process are investigated. Their water swelling ratio, free and bound water, and ion conductivity were investigated in an attempt to characterize hybrid membranes for future application of the hybrid as an ion-exchange membrane.

EXPERIMENTAL

Preparation of hybrid membranes

The polymer used in this study was PVDF-HFP (KY-NAR 2801, Flex Atochem., Philadelphia, PA). It was dissolved in *N,N*-dimethylacetamide (DMAc) at room temperature to a concentration of 7 wt % and was stirred constantly to ensure homogeneity. A homogeneous TEOS (Aldrich Chem. Co., Milwaukee, WI) mixture was prepared using DMAc, hydrochloric acid, SSA (70 wt % solution in water, Aldrich Chem.

TABLE I
Experimental Conditions of Polymer Solutions

Sample	PVDF (wt %)	TEOS (wt %)	TEOS (mmol)	H ₂ O (mmol)	SSA wt % (H ₂ O mmol)
PT 0	7	0	0	0	0
PTS 10	7	10	1.87	0	11.3 (7.48)
PTS 20	7	20	4.2	0	22.3 (16.8)
PTS 30	7	30	7.2	0	33.1 (28.8)
PTS 40	7	40	11.2	0	43.4 (44.8)
PT 20	7	20	4.2	16.8	0
PT 30	7	30	7.2	28.8	0

Co.), and TEOS. This solution was prepared by mixing H₂O/HCl/TEOS in a molar ratio of 4/0.1/1. H₂O in SSA was used in the sol-gel process. The TEOS solution was dropped into the PVDF-HFP solution while stirring to form homogeneous mixtures, which were then stirred at room temperature for 12 h. The homogeneous solution was poured into a petri dish. After drying at 60°C for 12 h and 130°C for 12 h, respectively, the PVDF-HFP/SiO₂/SSA hybrid film (named PTS n) was obtained. In addition, the PVDF-HFP/SiO₂ hybrid films without SSA were prepared using pure water (named PT n). The experimental conditions for the polymer solutions are given in Table I. For comparison, amorphous silica particles were synthesized by the addition, under vigorous stirring, of TEOS to a solution of ethanol and the stoichiometric amount of water and 0.1M HCl. The solution was mixed at room temperature for 12 h before drying.

Characterization

²⁹Si-NMR provides a unique way of confirming the hydrolysis and condensation reactions in the sol-gel process. As the polymerization progressed, distinct resonance were observed for the silicon units with Q⁰ through Q⁴ species (increasing the extent of condensation), where the superscript refers to the number of -O-Si groups bonded to the silicon atom of interest.¹⁸ The ²⁹Si solid-state spectra of selected samples were recorded on a Varian Unity Inova spectrometer at 300 MHz (Varian model NMR 1000 spectrometer, Varian Inc., Palo Alto, CA) using the magic angle spinning technique. The sample was located in a zirconia rotor operating at a spinning rate of 3.5 kHz. The spectral width was 50 kHz, and 64 k data points were used. Acquisition time of 0.064 s and a relaxation delay of 10 s were used. The chemical shifts are given with reference to tetramethylsilane.

FT-IR spectra of membranes were measured by Nicolet IR 760 spectra E.S.P (Thermo Nicolet, WI) in the 4,000–500 cm⁻¹ ranges. To investigate the morphology of films, fracture surfaces were investigated by field emission scanning electron microscope (FE-

SEM, Jeol Model JSF 6340F, Kyoto, Japan). All the films were gold coated and mounted on aluminum mounts with carbon paste.

The process of degradation and thermal stability of films were monitored by thermogravimetric analysis (TGA, Instruments, DE). The TGA measurements were carried out under a nitrogen atmosphere at a heating rate of 10°C/min from 50 to 700°C.

The DSC measurements were carried out using a DSC 2010 thermal analyzer (TA, Instruments) equipped with a cooling apparatus. In the measurement, the nonfreezing water of the wet sample was determined by DSC. About 5 mg of a PVA sample swollen with water was placed and sealed in an aluminum pan, which had been pretreated in boiling water for 1 h to eliminate the reaction of water with the aluminum surface during DSC runs. After cooling with liquid nitrogen, the experiment was started by heating from -50 to 50°C at a rate of 5°C/min. Nitrogen gas was used as the carrier gas with a flow rate of 200 mL/min.

The wide-angle X-ray diffraction (WAXD) patterns were recorded by the reflection scan with nickel-filtered Cu K α radiation using the X-ray diffractometer (Rigaku Denki Model RAD-C, Rigaku, Kyoto, Japan). The X-ray generator was run at 40 kV and 100 mA. All the WAXD measurements were performed at 2 θ between 5 and 50°.

Dynamic vapor sorption and measurement of water swelling ratio

Water vapor sorption experiments were carried out using a dynamic vapor sorption apparatus (DVS-1000, Surface Measurement Systems Ltd., London, UK) at 90% relative humidity (RH). The water swelling ratio was measured as follows.

After soaking the samples in distilled water for more than 24 h in the temperature range from 40 to 80°C, they were wiped with filter paper and weighed immediately. The samples were then dried under vacuum until a constant weight was obtained. The water swelling ratio was determined by the following equation:

$$\text{Water swelling ratio} = \frac{W_{\text{wet}} - W_{\text{dry}}}{W_{\text{dry}}} \quad (1)$$

where, W_{wet} and W_{dry} are wet and dried membrane weight, respectively.

Ion conductivity measurement

Proton conductivity in membranes is normally measured with a four-point probe technique. The impedance of membrane was determined by a Full Material Impedance System 12608W consisting of a Frequency

Response Analyzer 1260 and an Electrochemical Interface 1287 (Solatron Analytical, Berks, UK). Each sample for the measurement was prepared with a surface area of 4 × 1 cm and a membrane thickness of 100 to 150 μm . The ion conductivity (σ) was obtained by the following equation:

$$\sigma = \frac{l}{R \times S} \quad (2)$$

where σ is the proton conductivity (S/cm), l is the membrane thickness (cm), R is the resistance (Ω), and S is the surface area for the ion to penetrate through (cm^2).

Mechanical property

Mechanical properties of the membranes were evaluated using an Instron testing machine (Model 4465 with 1 kN load cell, MA) and analyzed in accordance with the ASTM D882-91 standard test protocol for thin film tensile tests. All the tests were conducted at a crosshead speed of 10 mm/min. Ten specimens of each tensile sample were tested to provide assurance of good data reproducibility. The percentage strain (λ) was calculated as follows:

$$\lambda = [(L - L_0)/L_0] \times 100 \quad (3)$$

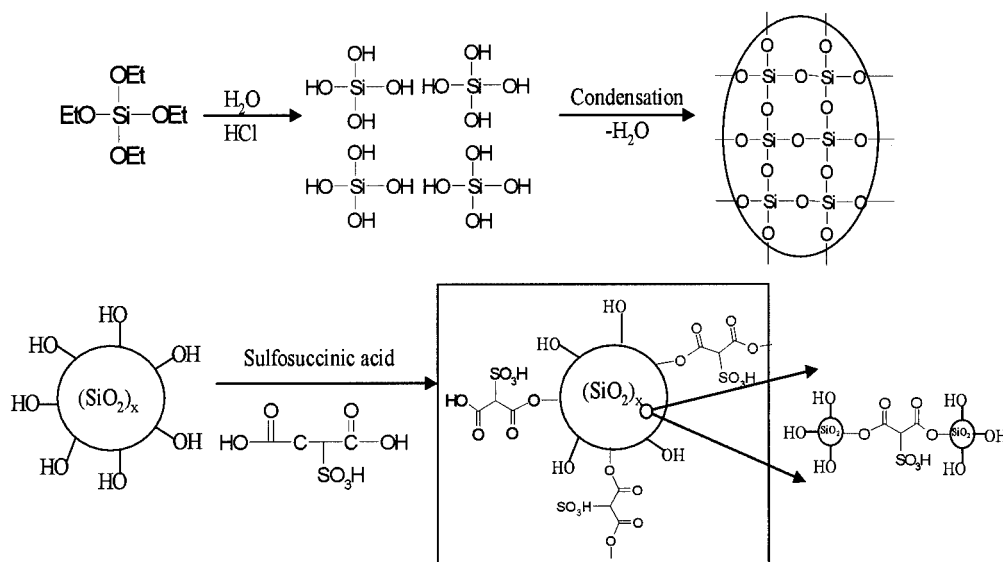
where L is the total extension measured from the grip displacement and L_0 is the grip distance (20 mm). The initial Young's modulus (E) was calculated from the initial slope of the stress-strain curve obtained. The tensile strength was recorded as stress at ultimate fracture.¹⁹

RESULTS AND DISCUSSION

Sample preparation

Organic-inorganic hybrids were prepared using PVDF-HFP, sulfosuccinic acid, and TEOS via the sol-gel process involving hydrolysis and polycondensation of TEOS. PVDF can also hydrogen bond between F atoms from PVDF and H atoms from silanol and be incorporated with inorganic minerals.⁶ The hybridization of TEOS and SSA proceeds through an esterification reaction between the silanol groups of hydrolyzed TEOS and carboxylic groups of SSA. Scheme 1 shows the postulated reaction mechanism of sulfosuccinic acid with hydrolyzed TEOS.

The proportion of TEOS and SSA in the matrix varied from 0 to 40 wt % and 0-43.4 wt %, respectively. PT20 and PT30 without SSA were used as references. The membranes became opaque when the TEOS content was more than 30 wt %.



Scheme 1 Postulated reaction mechanism of sulfosuccinic acid with hydrolyzed TEOS.

^{29}Si solid-state NMR spectroscopy

Figure 1 shows representative ^{29}Si solid-state NMR spectra for the hybrid materials. As the hydrolysis and condensation proceed, five coordination states around the Si atoms can be distinguished, each state designated using the Q^n notation. Maciel and Sindorf²⁰ have reported that acid-catalyzed TEOS gel contained approximately equal amounts of Q^3 and Q^4 species, whereas the base catalyzed gel had a larger proportion of Q^4 species. For PVDF/silica hybrid materials (PT30), the percentage of Q^2 and Q^3 species was calculated to be 14.52 and 26.33%, respectively, as seen in Table II. However, for PVDF/silica/SSA hybrid membrane (PTS30), the percentage of Q^2 and Q^3 species was reduced to 0 and 17.72%, respectively. These residual OH groups in PT30 provide the reactive sites for the carboxylic acid group of sulfosuccinic acid and/or the polymer matrix through an esterification reaction and hydrogen bonding, respectively, resulting in homogeneous films.

IR spectroscopy

FT-IR spectroscopy was used to study the chemical structure of the hybrid membranes containing various proportions of silica. As shown Figure 2, the pure silicate shows a characteristic band at 772 cm^{-1} (symmetric Si–O–Si stretching), $1,048$ and $1,220\text{ cm}^{-1}$ (asymmetric Si–O–Si stretching), and 942 cm^{-1} (Si–OH stretching). Typical PVDF (PT0) bands appear at 879 cm^{-1} (CF_2 symmetric stretching) and 838 cm^{-1} (CH_2 rocking).

The hybrid membranes (PTS30) with sulfosuccinic acid show the characteristic ester absorption band at $1,725\text{ cm}^{-1}$ ($\text{C}=\text{O}$, sulfosuccinic acid), which is not

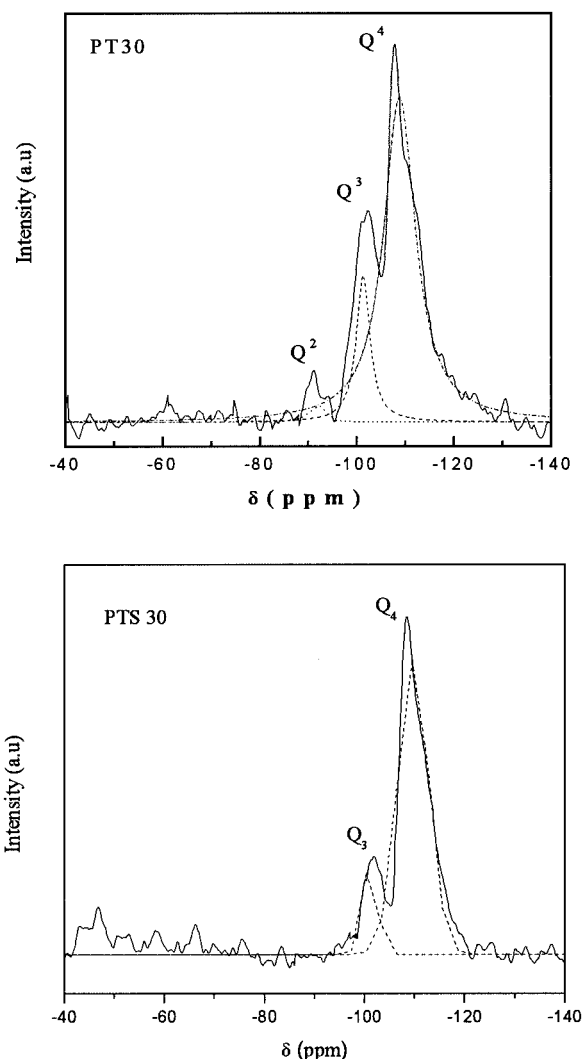


Figure 1 ^{29}Si solid-state NMR spectra of PT30 and PTS30. The dashed lines are calculated by the best-fit contributions assuming 90% Lorentzian–Gaussian peaks.

TABLE II
Results of Peak Deconvolution in ^{29}Si Solid-State NMR

Sample	Si spectra (at %)	
	PT 30	PTS 30
Q^0 (-71 to -78 ppm) ^a	0	0
Q^1 (-81 to -88 ppm)	0	0
Q^2 (-89 to -95 ppm)	14.52	0
Q^3 (-98 to -105 ppm)	26.33	17.72
Q^4 (-106 to -121 ppm)	59.15	82.28

^a From Brinker and Scherer⁸

present in the spectrum of hybrid membranes without SSA (PT30). The absorption band assigned to the sulfonic acid group was observed at $1,200\text{ cm}^{-1}$ (S=O asymmetric stretch), $1,045\text{ cm}^{-1}$ (S=O symmetric stretch), and 687 cm^{-1} (S-O stretch). This showed that the esterification reaction was complete. In addition, the peak at 945 cm^{-1} (Si-OH stretching) in silicate and a broad band at $1,048\text{--}1,220\text{ cm}^{-1}$ (Si-O-Si asymmetric stretching) are seen in the spectra of the hybrid (PTS30). In the spectra of the PTS30 hybrid membrane both characteristic FT-IR bands for SiO_2 , PVDF-HFP, and SSA were present, indicating that hybridization was achieved via the sol-gel reaction. The broad absorption peak at around $3,500\text{ cm}^{-1}$ in the hybrid materials indicates that there is a significant amount of OH group left. These noncondensed OH groups provided the sites for hydrogen bonding between PVDF and hydrated silicates and/or SSA, resulting in the homogeneous membranes.

Scanning electron microscopy (SEM)

Figure 3 shows SEM images of the hybrid membranes. In the case of a hybrid membrane containing SSA (PTS30), silica microparticles and the voids are observable. The silica microparticle was confirmed by energy-dispersive X-ray analysis (EDXA). Comparing the PTS30 hybrid membrane containing SSA, the PT30 hybrid membrane without SSA did not show any voids. This is presumably due to repulsion between hydrophobic PVDF and hydrophilic sulfosuccinic acid in the case of PTS30 and strong interaction between PVDF and silica in the case of PT 30.

Wide-angle X-ray diffraction

The structural change produced by the presence of silica domains was further characterized with WAXD. WAXD patterns of hybrids were compared with that of PVDF-HFP (PT0). In general, when a polymer contains a large crystalline region, the X-ray diffraction peak is sharp and the intensity is large, whereas that of an amorphous polymer is rather broad.²¹ According to X-ray diffraction measurements shown in Figure 4, pure PVDF membrane showed diffraction peaks at around $2\theta = 20.05, 36.5,$ and 39.05° because of the existence of form I crystals of the ferroelectric all-*trans* phase.⁴ Although the locations of corresponding hybrid peaks did not shift on the incorporation of silicate, the X-ray diffraction peak was broadened as the silica content increased, meaning an increase of the amorphous region in the hybrid.

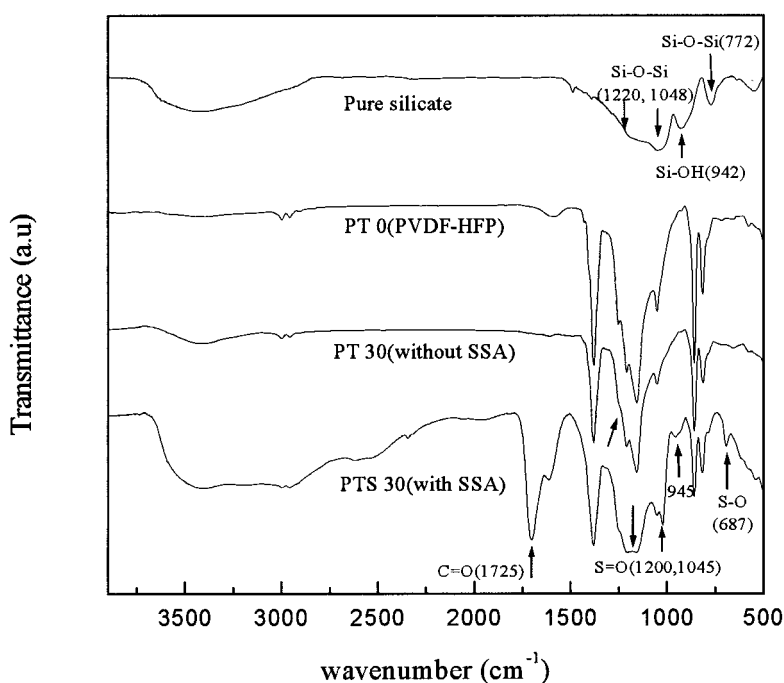


Figure 2 FT-IR spectra of hybrid membranes.

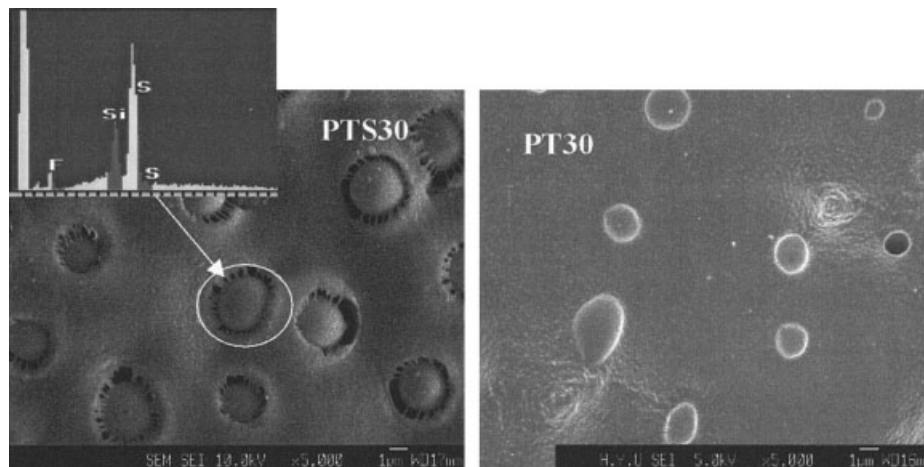


Figure 3 SEM micrograph and EDXA of the membranes.

Thermal analysis

The TGA curves of hybrid materials under nitrogen are shown in Figure 5 and the results are summarized in Table III. The TGA curve of the hybrids can be fitted by three main degradation steps. A continuous weight loss occurred at low temperature in the membrane containing silica because of the release of water. Besides the thermal stability of the hybrid membranes, the water-polymer interaction was investigated by thermal analysis. The temperature at which water evaporated from the membrane was measured by the weight decrease in the TGA curve. Compared with the hybrid membrane without SSA, the hybrid membrane containing SSA has a higher concentration of water in

the polymer matrix, while the water content is proportional to the content of SSA. Those water molecules evaporate above 100°C. Most of the water molecules in the hybrid membrane having SSA are supposed to exist in a bound state rather than in a free molecular state.²² The water molecules seem to be bound directly to the $-\text{SO}_3\text{H}$ of SSA. This behavior was confirmed by state of water in membrane using DSC and will be discussed in the following section.

Compared with PT0 and/or PT30 without SSA as a reference, the initial thermal decomposition temperature (T_{m1}) of the hybrid membranes containing sulfonic acid groups was about 240°C, which is attributed to desulfonation of the SSA. T_{m1} increases with silica and SSA content. This may be associated with the esterification between silica and SSA.

The maximum temperature of the rate of weight loss (T_{m2}) was about 470°C, which was attributed to the decomposition of the PVDF. T_{m2} of the hybrid membranes shifted to a lower temperature with increasing silica content.

In the case of composite films, the weight remaining after decomposition is dependent on the amount of the inorganic component as shown in Figure 5(b). That is, the weight residue of composites at 700°C increases with increasing TEOS content. These results suggest that the introduction of silica into the PVDF chain clearly enhances the thermal stability of the given hybrid materials.

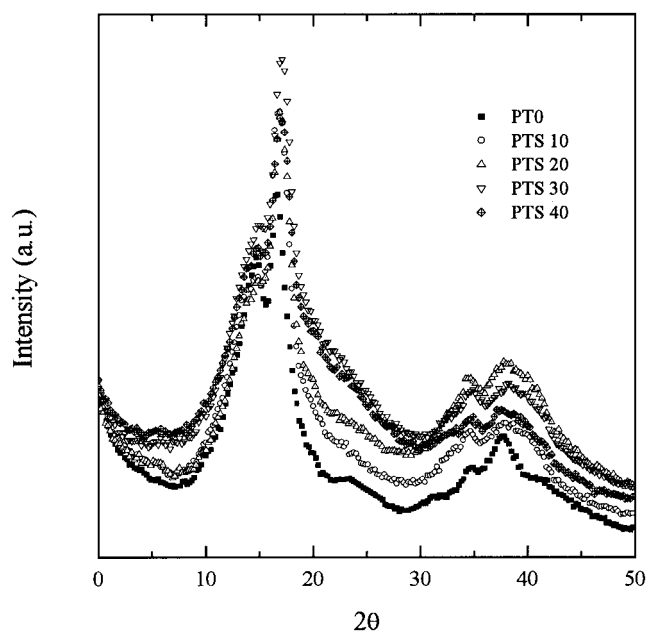


Figure 4 X-ray diffractograms of pure PVDF-HFP (PT0) and hybrid membranes.

States of water in membranes and water vapor sorption

The sorption behavior of water for the prepared membranes was investigated by measuring their equilibrium water content. The water vapor sorption of prepared membranes under RH 90% at room temperature is shown in Figure 6. The water absorption behavior of

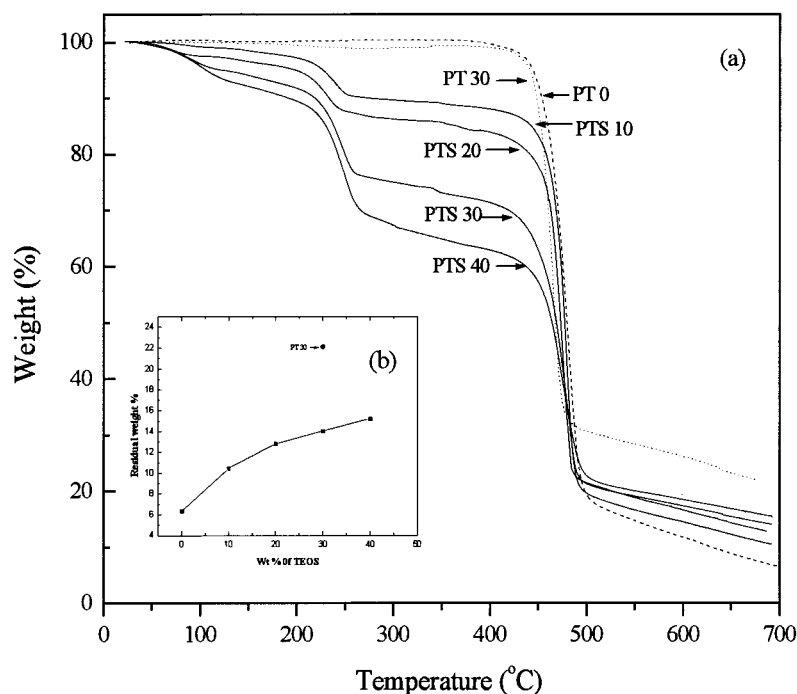


Figure 5 (a) TGA curves. (b) Residual weight percent of membranes at 700°C.

hybrid membranes is different from that of PVDF membranes. Incorporation of silica and SSA affected the water absorption behavior. The water molecules in hybrid membranes showed relatively strong interactions with the sulfonic acid groups of SSA. The vapor sorption increases with TEOS and SSA content. Generally, the water in the polymer engaged in strong interactions with the ionic component of the polymer. These interactions overcome the strong tendency of the polymer to exclude water due to its hydrophobic nature and resistance to swelling.

Figure 7 shows the swelling behavior of hybrid membranes. The swelling of PVDF-HFP/SiO₂/SSA hybrid membranes (PTS10-PTS40) depends on the content of charged groups ($-\text{SO}_3^-$) and TEOS, whereas the swelling of PVDF/SiO₂ hybrid mem-

branes (PT20, PT30) depends on the content of TEOS. Note that the swelling of hybrid membranes is independent of the temperature.

Various terms have been used to characterize the water associated with hydrophilic polymers. In general, the states of water in a polymer can be distinguished into free water, freezing water, and nonfreezing water.²² Free water is the water that has the same phase transition temperature as bulk water (0°C).²³ Freezing water is defined as the water that has a phase

TABLE III
Characteristic Parameters of Thermal Degradation for Hybrid Membranes

Sample	T_{m1} ^a	T_{m2}	Ash ^b
PT 0	-	480	6.5
PTS 10	241	478	10.4
PTS 20	243	478	12.8
PTS 30	247	477	14.1
PTS 40	249	475	15.2
PT 30	-	474	22

^a T_{m1} and T_{m2} are the maximum rate temperature of weight loss corresponding to the decomposition of the SSA and PVDF, respectively.

^b Residual ash is the char yield (wt %) at 700°C.

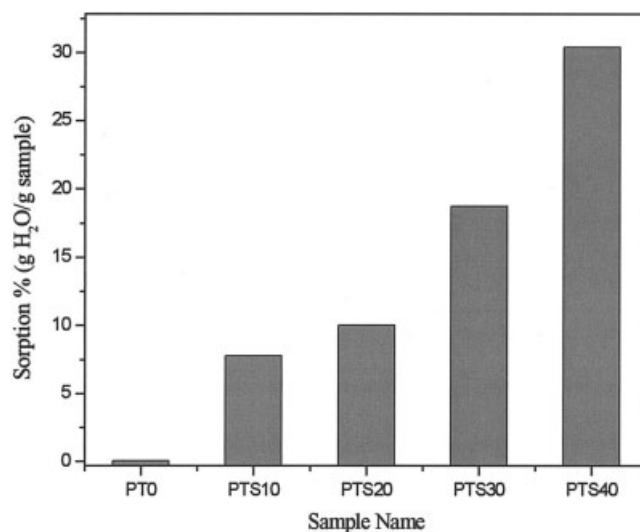


Figure 6 Water vapor sorption of prepared membranes under RH 90%.

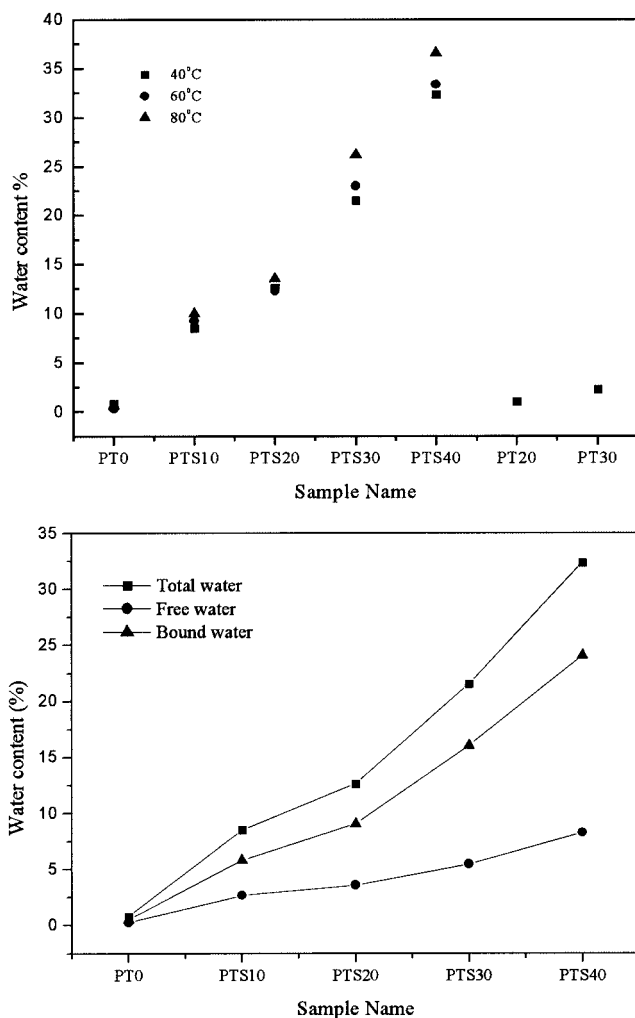


Figure 7 State of water in membrane.

transition temperature lower than 0°C due to weak interaction with the polymer. Nonfreezing water is the water that has no detectable phase transition from -73 to 0°C due to strong interaction with the polymer.²³ When the frozen membrane sample is heated in a calorimeter, the heat required to melt the frozen water can be measured. Nonfreezing water, which is defined as the bound water, is the difference between the total water and the frozen water.

In this study, DSC measurement was used to determine the amount of free water that is not bound by hydrogen bonding. Table IV and Figure 7 show the content of water correspond to free and bound water as well as total water as a function of SSA concentration. The water content of the membranes decreased in the order bound water > free water. Free and bound water contents were dependent upon the total water content of the membranes, indicating water states in the polymer are very different with the polymer structure. Bound water increased with SSA content. This result was conformed to weight loss of TGA.

As listed in Table IV, the hybrid membranes without SSA (PT20, PT30) have not shown free water indicating an induced silica to make the membranes structure more rigid and compact due to strong interaction with PVDF and silica. However, the hybrid membranes containing SSA have free volume due to repulsion between hydrophobic PVDF and hydrophilic sulfosuccinic acid.

Ion conductivity

Figure 8 shows the change in the ion conductivity of hybrid membranes with increasing SSA concentration. The ion conductivity of hybrid membranes measured at 25 and 50°C are in the range between 10^{-6} and 10^{-4} S/cm. The conductivity increased with the increase of SSA content and water content due to the increase of carrier ions ($-\text{SO}_3\text{H}$) and the formation of a hydrogen bridge between charged groups. The ion conductivity increases slightly with temperature. Usually, ionic mobility increases as more water and ion exchange sites are introduced into the membrane.²⁵

Mechanical property

Figure 9 describes the stress-strain results obtained on the hybrid membranes as well as for the pure PVDF membrane. Specific values of the mechanical properties of hybrid membranes are summarized in Table V. Figure 9(a) describes the stress-strain results obtained for the hybrid membrane without SSA (PT20, PT30) as well as for the pure PVDF-HFP membrane (PT0). The yield stress tended to increase slightly with TEOS content. The effect of TEOS content on the tensile modulus was also similar to that on yield stress. The yield strain and elongation of the hybrids decreased markedly with increasing TEOS content, as seen in Figure 9(a) and Table V. Hybrids with a small amount of silica exhibited a drastic improvement in mechanical properties for two reasons: (1) silica disperses

TABLE IV
State of Water in Membranes

Sample	Total water (%)	Free water (%)	Bound water (%)
PT 0	0.8	0.3	0.5
PTS 10	8.5	2.7	5.8
PTS 20	12.6	3.6	9.0
PTS 30	21.5	5.5	16.0
PTS 40	32.4	8.3	24.1
PT 20	0.9	0	0.9
PT 30	2.3	0	2.3

Free water content (%) in total water = (endothermic peak area at around 0°C in water-swollen polymer)/(melting endothermic heat of fusion (J/g) for pure water (334 J/g²⁴) × total water content (%).

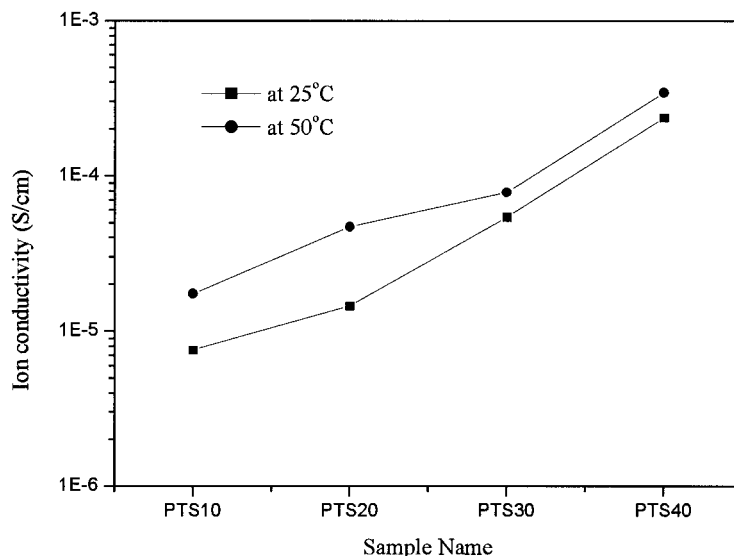


Figure 8 Ion conductivity for hybrid membrane with SSA concentration.

evenly throughout the polymer matrix, and (2) the polymer chain strongly interacts with silica or silanol through hydrogen bonding. The mechanical properties of hybrid membranes without SSA show the reinforcing effect in strength through the homogeneous dispersion of the micro-SiO₂ particles in the polymer matrix. On the other hand, the mechanical behavior of the hybrid membranes with SSA was very different from that of the hybrid membranes without SSA. In comparison with pure PVDF, hybrid membranes containing SSA have a lower Young's modulus and lower yield stress, but a higher yield strain and higher breaking elongation. Yield stress and modulus decreased with SSA content. The yield strain and breaking elongation tended to increase slightly with SSA content, as shown in Figure 9(b) and Table V.

As reported,²⁶ the stress should be reduced if there are no bonding sites between the organic polymer phase and the inorganic phase. This is presumably due to the weak interactions between these polymers and the inorganic phase. In our case, an abrupt reduction of yield stress and modulus is believed to result from the weak interactions between PVDF and the SSA with higher SSA content.

CONCLUSION

Organic-inorganic hybrids, based on PVDF-HFP/SiO₂ hybrid membranes containing sulfonic acid groups, were prepared via *in situ* polymerization of TEOS and SSA using the sol-gel process. The hybridization of TEOS and SSA proceeds through an esterification reaction between the silanol groups of the hydrolyzed TEOS and carboxylic acid groups of SSA. FT-IR analysis confirmed the chemical structure of the

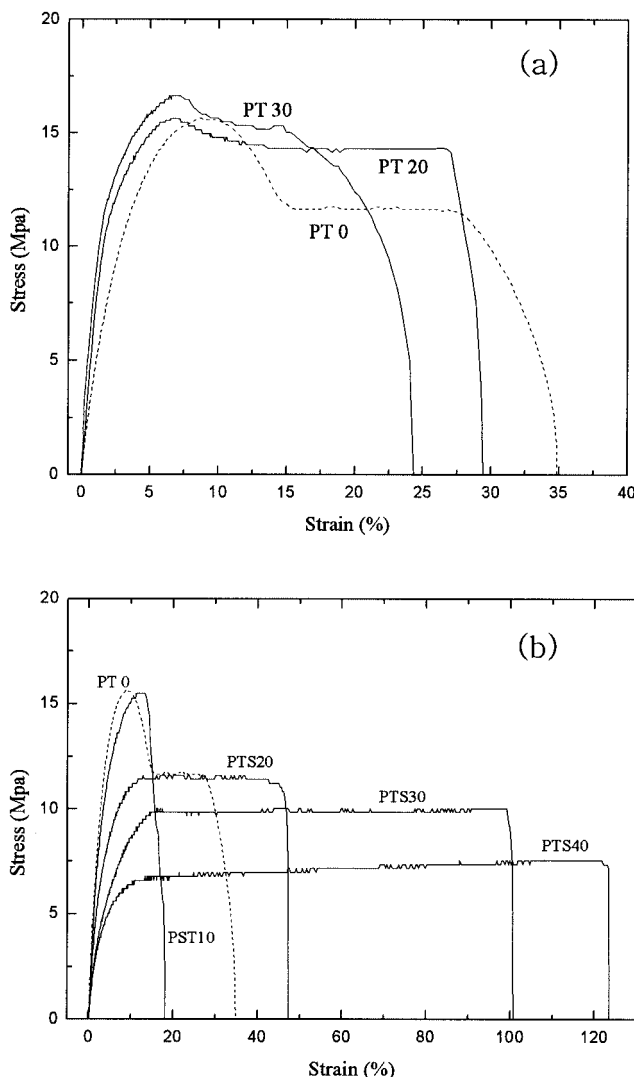


Figure 9 Stress-strain curves of pure PVDF-HFP (PT0) and hybrid membranes.

TABLE V
Mechanical Properties of Hybrid Membranes

Sample	Modulus (Mpa)	Yield stress (Mpa)	Yield strain (%)	Breaking elongation (%)
PT 0	507.8	15.5	9.78	35
PTS 10	497	15.4	11.82	19
PTS 20	343.7	12.17	12.83	47
PTS 30	286.9	9.84	14.6	104.7
PTS 40	273.3	6.4	15.35	123
PT 20	667.3	15.63	7.33	29
PT 30	702.6	16.64	6.53	24

PVDF-HFP/silica/SSA hybrid. The X-ray diffraction peak is broadened as the silica content increases, indicating an increase in the amorphous region in the hybrid. The membranes containing more sulfonic acid groups showed a higher vapor sorption and swelling behavior. Most of the water molecules in the hybrid membrane with SSA are supposed to exist in a bound state rather than in a free molecular state. The water molecules seem to be bound directly to the $-\text{SO}_3\text{H}$ of SSA. The ion conductivity of the membrane is proportional to the SSA concentration. Silica content in the hybrid membrane without SSA had great effect on mechanical properties: tensile modulus and yield stress increased and yield strain and elongation at break decreased with increased silica content. However, in the case of the hybrid membrane containing SSA, modulus and yield stress decreased and yield strain and elongation at break increased with increased silica content due to the weak interactions between the hydrophobic polymer chain and the hydrophilic group of SSA. Overall, the technique of introducing a chemical bond between inorganic/organic materials is an important and useful means to improve the properties of hybrid membranes.

This study was completed for the Carbon Dioxide Reduction and Sequestration Center, one of the 21st Century Frontier R and D Programs funded by the Ministry of Science and

Technology of Korea. Dae Sik Kim was the recipient of a scholarship from the BK 21 Program of Hanyang University.

References

- Judeinstein, P.; Sanchez, C. J. *Mater Chem* 1996, 6, 511.
- Neoh, K. G.; Tan, K. K.; Goh, P. L.; Huang, S. W. Kang, E. T.; Tan, K. L. *Polymer* 1999, 40, 887.
- Imai, Y.; Naka, K.; Chujo, Y. *Macromolecules* 1998, 31, 532.
- Cho, J. W.; Sul, K. I. *Polymer* 2001, 42, 727.
- Yeom, S. H.; Chung, Y. S.; Lee, W. T.; Kim, S. I.; Kim, J. H. *Membrane J* 2001, 11, 116.
- Yano, S.; Iwata, K.; Kurita, K. *Mater Sci Eng* 1998, C6, 75–90.
- Jang, J.; Park, H. *J Appl Polym Sci* 2001, 85, 2074–2083.
- Brinker, C. J.; Scherer, G. W. *Sol-Gel Science: The Physics and Chemistry of Sol-Gel Processing*; Academic Press, San Diego, 1999.
- Park, H. B.; Kim, J. H.; Lee, Y. M. *Macromol Rapid Commun* 2002, 23, 544.
- Park, H. B.; Kim, J. K.; Nam, S. Y.; Lee, Y. M. *J Membr Sci* to appear.
- Saegusa, T. J. *Macromol Sci Chem* 1991, A28, 817.
- Chujo, Y.; Ihara, E.; Kure, S.; Suzuki, K.; Saegusa, T. *Macromol Chem Macromol Symp* 1991, 303, 42.
- Nalwa, H. S. *Ferroelectric Polymers: Part 1*; Marcel Dekker, New York, 1995.
- Ueda, M.; Toyota, H.; Ouchi, T.; Sugiyama, J. I.; Yonetake, K.; Masuko, T.; Teramoto, T. *J Polym Sci Part A* 1993, 31, 853.
- Blanco, J. F.; Nguyen, Q. T.; Schaetzl, P. *J Membr Sci* 2001, 186, 267.
- Park, H. B.; Nam, S. Y.; Rhim, J. W.; Lee, J. M.; Kim, S. E.; Kim, J. R.; Lee, Y. M. *J Appl Polym Sci* 2002, 86, 2611.
- Yoshikawa, M.; Tsubouchi, K.; Guiver, M. D.; Robertson, G. P. *J Appl Polym Sci* 1999, 74, 407–412.
- Engelhardt, G.; Michel, D. *High Resolution Solid State NMR of Silicate and Zeolites*; Wiley, New York, 1987.
- Genies, C.; Mercier, R.; Sillion, B.; Petiaud, P.; Cornet, N.; Gebel, G.; Pineri, M. *Polymer* 2001, 42, 5097.
- Maciel, G. A.; Sindorf, D. W. *J Am Chem Soc* 1980, 102, 7606.
- Kim, J. H.; Lee, Y. M. *J Membr Sci* 2001, 193, 209.
- Nakamura, K.; Hatakeyama, T.; Hatakeyama, H. *Textile Res J* 1981, September, 607–613.
- Higuchi, A.; Iijima, T. *Polymer* 1985, 26, 1207.
- Samuel, P. K.; Sano, K.; Sudoh, M.; Kensaka, M. *Sep Purif Tech* 2000, 18, 141–150.
- Honma, I.; Nishikawa, O.; Sugimoto, T.; Nomura, S.; Nakajima, H. *Fuel Cells* 2002, 1, 52.
- Chen, Y.; Jude, O. *Chem Mater* 1999, 11, 1218.